



UNIVERSITY OF LEEDS

This is a repository copy of *Metagenomic and 14 C tracing evidence for autotrophic microbial CO2 fixation in paddy soils.*

White Rose Research Online URL for this paper:
<https://eprints.whiterose.ac.uk/165325/>

Version: Accepted Version

Article:

Xiao, K orcid.org/0000-0001-6809-9340, Ge, T, Wu, X et al. (6 more authors) (2021) Metagenomic and 14 C tracing evidence for autotrophic microbial CO2 fixation in paddy soils. *Environmental Microbiology*, 23 (2). pp. 924-933. ISSN 1462-2912

<https://doi.org/10.1111/1462-2920.15204>

© 2020 Society for Applied Microbiology and John Wiley & Sons Ltd. This is the peer reviewed version of the following article: Xiao, K, Ge, T, Wu, X et al. (6 more authors) (2020) Metagenomic and 14 C tracing evidence for autotrophic microbial CO2 fixation in paddy soils. *Environmental Microbiology* which has been published in final form at 10.1111/1462-2920.15204. This article may be used for non-commercial purposes in accordance with Wiley Terms and Conditions for Use of Self-Archived Versions.

Reuse

Items deposited in White Rose Research Online are protected by copyright, with all rights reserved unless indicated otherwise. They may be downloaded and/or printed for private study, or other acts as permitted by national copyright laws. The publisher or other rights holders may allow further reproduction and re-use of the full text version. This is indicated by the licence information on the White Rose Research Online record for the item.

Takedown

If you consider content in White Rose Research Online to be in breach of UK law, please notify us by emailing eprints@whiterose.ac.uk including the URL of the record and the reason for the withdrawal request.



eprints@whiterose.ac.uk
<https://eprints.whiterose.ac.uk/>



Metagenomic and ^{14}C tracing evidence for autotrophic microbial CO_2 fixation in paddy soils

Journal:	<i>Environmental Microbiology and Environmental Microbiology Reports</i>
Manuscript ID	EMI-2020-1232
Journal:	Environmental Microbiology
Manuscript Type:	EMI - Special Issue Article
Date Submitted by the Author:	30-Jul-2020
Complete List of Authors:	Xiao, Ke-Qing; University of Leeds, School of Earth and Environment Zhu, Yong-Guan; Chinese Academy of Sciences, Res Ctr Eco-environ Sci; Chinese Academy of Sciences, Institute of Urban Environment Ge, Tida; the Chinese Academy of Sciences (CAS), Institute of Subtropical Agriculture (ISA)
Keywords:	Autotrophic microbes, marker gene,, soil organic carbon, paddy soil

SCHOLARONE™
Manuscripts

1 **Metagenomic and ¹⁴C tracing evidence for autotrophic**
2 **microbial CO₂ fixation in paddy soils**

3 Ke-Qing Xiao¹, Ti-Da Ge², Xiao-Hong Wu³, Caroline L. Peacock¹, Zhen-Ke Zhu²,
4 Jingjing Peng⁴, Peng Bao⁵, Jin-Shui Wu², Yong-Guan Zhu^{5 6 *}

5 ¹School of Earth and Environment, University of Leeds, Leeds LS2 9JT, UK; ²Key
6 Laboratory of Agro-ecological Processes in Subtropical Region & Changsha
7 Research Station for Agricultural and Environmental Monitoring, Institute of
8 Subtropical Agriculture, Chinese Academy of Sciences, Hunan 410125, China;
9 ³National Engineering Laboratory of Applied Technology for Forestry & Ecology in
10 Southern China, Central South University of Forestry and Technology, Changsha
11 410004, Hunan, China; ⁴College of Resources and Environmental Sciences, China
12 Agricultural University, Beijing, 100193, China; ⁵Key Lab of Urban Environment and
13 Health, Institute of Urban Environment, Chinese Academy of Sciences, 1799 Jimei
14 Road, Xiamen, 361021, China; ⁶State Key Laboratory of Urban and Regional Ecology,
15 Research Center for Eco-Environmental Sciences, Chinese Academy of Sciences, 18
16 Shuangqing Road, Beijing, 100085, China;

17
18 Running title: Autotrophic microbial CO₂ fixation in paddy soil

19
20 * Corresponding author

21 Address: State Key Laboratory of Urban and Regional Ecology, Research Center for
22 Eco-Environmental Sciences, Chinese Academy of Sciences, 18 Shuangqing Road,
23 Beijing, 100085, China.

24 Phone: 86-10-6293 6940

25 Fax: 86-10-6293 6940

26 Email: ygzhu@rcees.ac.cn

27 **Originality-Significance Statement**

28 The role of autotrophic carbon fixation in SOC formation is unclear to date. This study
29 detects marker genes from all known autotrophic pathways in paddy soils for the first
30 time using metagenomic analysis. ^{14}C -labelling experiment shows that autotrophic
31 microbes are active and contribute significantly to the stable SOC pool. Our work
32 highlights the importance of microbial CO_2 fixation to SOC accumulation in paddy
33 soils.

34 **Summary**

35 Autotrophic carbon dioxide (CO_2) fixation by microbes is ubiquitous in the
36 environment and potentially contributes to the soil organic carbon (SOC) pool.
37 However, the multiple autotrophic pathways of microbial carbon assimilation and
38 fixation in paddy soils remain poorly characterized. In this study, we combine
39 metagenomic analysis with ^{14}C -labelling to investigate all known autotrophic
40 pathways and CO_2 assimilation mechanisms in five typical paddy soils from southern
41 China. Marker genes of six autotrophic pathways are detected in all soil samples,
42 which are dominated by the *cbbL* genes (67-82%) coding the ribulose-bisphosphate
43 carboxylase large chain in the Calvin cycle. These marker genes are associated with
44 a broad range of phototrophic and chemotrophic genera. Significant amounts of
45 ^{14}C - CO_2 are assimilated into SOC (74.3 to 175.8 mg ^{14}C kg $^{-1}$) and microbial biomass
46 (5.2 to 24.1 mg ^{14}C kg $^{-1}$) after 45 days incubation, where more than 70% of ^{14}C -SOC
47 was concentrated in the relatively stable humin fractions. These results show that
48 paddy soil microbes contain the genetic potential for autotrophic carbon fixation
49 spreading over broad taxonomic ranges, and can incorporate atmospheric carbon into
50 organic components, which ultimately contribute to the stable SOC pool.

51 **Introduction**

52
53
54 Soil is the second largest pool of carbon on Earth, with 2000 Pg C in the form of

55 soil organic carbon (SOC) (Janzen, 2004). Soil organic carbon provides an important
56 source of carbon for microbial growth (Schimel and Schaeffer, 2012; Lehmann and
57 Kleber, 2015) and as part of soil organic matter supplies nutrients such as
58 phosphorus, sulfur, calcium, magnesium, and trace elements (Kapkiyai et al., 1999;
59 Dincher et al., 2020), which all contribute to the creation and maintenance of healthy
60 soils that are able to perform a wide range of ecosystem services (Schmidt et al.,
61 2011). The production and degradation of SOC also modulates the sequestration or
62 release of CO₂ (Lal, 2008), and thus directly helps to regulate short-term climate and
63 potentially mitigate against current climate change (Davidson and Janssens, 2006).
64 Traditionally SOC is thought to derive mainly from plant detritus, but new research
65 now shows that organic carbon from microbial sources might be the main contributor
66 to SOC (Simpson et al., 2007; Kallenbach et al., 2016; Liang et al., 2017), with
67 microbial necromass contributing up to 50-80% of SOC (Liang et al., 2019). This new
68 work highlights the potential importance of soil microbes in producing and
69 subsequently controlling the fate of SOC. Heterotrophic microbes have two critical but
70 contrasting roles in controlling SOC: promoting release of C to the atmosphere
71 through their catabolic production of CO₂, and preventing release of C to the
72 atmosphere by transforming labile organic carbon into a more stable form through
73 anabolism (Schimel and Schaeffer, 2012; Liang et al., 2017). Autotrophic microbes
74 meanwhile can fix CO₂ from the atmosphere and synthesize this into microbial
75 biomass (MBC) (Yuan et al., 2012b; Ge et al., 2013), which directly contributes to the
76 SOC pool. Autotrophic metabolisms result in net C sequestration and can add to SOC
77 in a continuously iterative process of cell generation, population growth and death
78 (Liang and Balsler, 2011; Liu et al., 2016). To date however, the role of autotrophic
79 carbon fixation in SOC formation is unclear and remains to be elucidated.

80 The assimilation of CO₂ into organic material is quantitatively the most important
81 biosynthetic process on Earth (Berg et al., 2007), as autotrophs generate the biomass
82 on which all other organisms thrive (Thauer, 2007). Six autotrophic CO₂ fixation

83 pathways have been found in various environments to date: the Calvin cycle
84 (Bassham et al., 1950), the reductive tricarboxylic acid (rTCA) cycle (Evans et al.,
85 1966), the reductive acetyl-CoA pathway (Wood et al., 1986), the
86 3-hydroxypropionate / malyl-CoA cycle (Holo, 1989), and the 3-hydroxypropionate /
87 4-hydroxybutyrate and dicarboxylate / 4-hydroxybutyrate cycle (named together as
88 the 4-hydroxybutyrate cycle) (Berg et al., 2007; Huber et al., 2008). The enzymes
89 catalyzing difficult steps in a given pathway are usually conserved and act as key
90 enzymes (Berg, 2011), and the corresponding coding genes, often named as marker
91 genes (Lever, 2013), are commonly used in microbial ecological studies. [For example,](#)
92 [cbbL was used](#) for ribulose 1,5-bisphosphate carboxylase/oxygenase (RubisCO) of
93 the Calvin cycle (Alfreider et al., 2003; Selesi et al., 2005; Yuan et al., 2012a; Xiao et
94 al., 2014b), [acl](#) for the ATP citrate lyase, [oorA](#) for 2-oxoglutarate: acceptor
95 oxidoreductase in the rTCA pathway (Campbell et al., 2003; Campbell and Cary, 2004;
96 Xiao et al., 2014a), and [hcd](#) for the 4-hydroxybutyryl-CoA dehydratase of both of the
97 4-hydroxybutyrate cycle (Zhang et al., 2010). Despite the discovery of these [six](#)
98 pathways most studies only focus on one to two pathways (mainly the Calvin cycle),
99 and there is a lack of comprehensive understanding of these pathways due to
100 limitations of PCR primers, like bias or poor specificity. Metagenomics involves the
101 direct sequencing of DNA from the environment and thus allows the examination of
102 multiple biochemical pathways and associated processes, bypassing PCR primers,
103 and so it is not limited to studying individual pieces of the metabolic puzzle (Venter et
104 al., 2004; Mackelprang et al., 2011). With the development of high-throughput
105 sequencing techniques and a dramatic drop of sequencing prices, diversity analysis
106 based on metagenomes is now feasible, which can target all metabolic pathways in
107 soil and does not rely on the specificity and coverage of the primers used (Liu et al.,
108 2018; Ma et al., 2018). [Moreover, metagenomics allows us to specifically analyze or](#)
109 [explore functional groups, study gene function and even reconstruct whole microbial](#)
110 [genome from complex environment samples](#) (Tyson et al., 2004; Hultman et al., 2015;

111 [Lam et al., 2015; Anantharaman et al., 2016; Metcalf et al., 2016](#)).

112 Paddy soil is a common soil type in China and around the world, and is also an
 113 ideal model system for studying microbiological and biogeochemical processes
 114 (Liesack et al., 2000; Xiao et al., 2014a). In this study metagenomics and $^{14}\text{CO}_2$
 115 labelling approaches are used to determine the genomic and geochemical potential of
 116 multiple autotrophic metabolisms in paddy soils to assimilate and fix atmospheric CO_2
 117 into SOC. Soil physicochemical properties are used for statistical analyses to identify
 118 the key factors driving microbial CO_2 sequestration in paddy soils. With a systematic
 119 analysis of multiple autotrophic pathways and their activities in paddy soil, this work
 120 provides new insight into the role of autotrophic CO_2 fixation in SOC formation.

121

122 **Results**

123 **Marker genes of different autotrophic pathways in paddy soil**

124 Marker genes of [six](#) autotrophic pathways are detected in all samples (Fig. 1a):
 125 *cbbL* (Calvin cycle, coding ribulose-bisphosphate carboxylase large chain) 7.2-11.7
 126 ppm, *acI*A (rTCA cycle, coding ATP-citrate lyase alpha-subunit) 0.8-1.6 ppm, *acsA*
 127 (reductive acetyl-CoA pathway, coding carbon-monoxide dehydrogenase catalytic
 128 subunit) 0.7-1.9 ppm, *accA* (3-hydroxypropionate/methyl-CoA cycle, coding acetyl-CoA
 129 carboxylase carboxyl transferase subunit alpha) 0.02-0.1 ppm, and *hcd*
 130 (4-hydroxybutyrate cycle, coding 4-hydroxybutyryl-CoA dehydratase) 0.2-1.8 ppm.
 131 The gene *cbbL* dominates (67-82%) in all samples, while *accA* is always the lowest (<
 132 1%) (Fig. 1b).

133 **Fig. 1**

134 **Table 1**

135 **Autotrophic microbes in paddy soils**

136 [Diverse microbes associated with marker genes](#) are found for [six](#) autotrophic
 137 pathways in paddy soils (Tab. S1). There exists the highest diversity for *cbbL*, second
 138 for *acsA*, followed by *hcd* and *accA*, lowest for *acI*A (Tab. 1). In the Calvin cycle, there

139 are 80 associated genera, with 34 phototrophs (13-20%), 50 chemotrophs (69-78%)
 140 and 3 mixotrophs (both phototrophs and chemotrophs, 5-11%) - *Rhodopseudomonas*
 141 *palustris*, *Thiocystis violascens* and *Rhodobacter sphaeroides*. In the reductive citric
 142 acid cycle, these microbes are exclusively chemotrophs, dominated by *Nitrospira*
 143 *defluvii* (94-98%). In the reductive acetyl-CoA pathway, all 28 genera are
 144 chemotrophs, mainly anaerobes like sulfate-reducing bacteria, acetogenic bacteria
 145 and methanogens. All four genera involved in the 3-hydroxypropionate / methyl-CoA
 146 cycle are phototrophs- *Chloroflexus aggregans*, *Chloroherpeton thalassium*,
 147 *Erythrobacter litoralis* and *Roseiflexus* sp. RS-1. In the 4-hydroxybutyrate cycle, all
 148 detected genera involved belong to chemotrophic archaea, and are dominated by two
 149 ammonia oxidation archaea-*Nitrosopumilus koreensis* and *Nitrososphaera gargensis*.
 150 The co-occurrence patterns of autotrophic microbes of six pathways in paddy soils are
 151 shown by network inference (Fig. 2). The resulting network consists of 121 nodes and
 152 871 edges with an average node connectivity of 14. The clustering coefficient is 0.65,
 153 and the modularity index is 0.5 (values > 0.4), suggesting that the network has a
 154 modular structure (Newman, 2006). Microbes associated with the Calvin cycle and
 155 the reductive acetyl-CoA pathway dominate the network owing to high diversity (Tab
 156 1), and microbes associated with the same pathway are inclined to cluster together
 157 and have stronger connections.

158 Fig. 2

159 Evidence of $^{14}\text{C-CO}_2$ assimilation by soil

160 After 45 days incubation the amounts of $^{14}\text{C-CO}_2$ incorporated into the soil
 161 organic carbon ($^{14}\text{C-SOC}$) and microbial biomass ($^{14}\text{C-MBC}$) are determined.
 162 Significant amounts of $^{14}\text{C-SOC}$ and $^{14}\text{C-MBC}$ are recovered from soils incubated
 163 under $^{14}\text{CO}_2$ atmosphere (Fig. 3a). The amounts of $^{14}\text{C-SOC}$ and $^{14}\text{C-MBC}$ range from
 164 74.3 (JX) to 175.8 (LZ) mg kg^{-1} and from 5.2 (YT) to 24.1 (TY-G) mg kg^{-1} , respectively,
 165 and $^{14}\text{C-MBC} / ^{14}\text{C-SOC}$ varies between 3.4% (LZ) and 24.9% (TY-G). The
 166 differences between soils in terms of incorporation into SOC and MBC vary

167 significantly between some paddy soils ($P < 0.05$). The calculated rates of CO₂
168 assimilation into SOC in paddy soils are 34.2-62.2 mg C m⁻² d⁻¹ (Fig. 3b). The total Fe,
169 clay and sand contents, and abundances of *cbbL* are significantly ($P < 0.05$)
170 correlated with the amounts of ¹⁴C-SOC in paddy soils (Tab. 2).

171 **Fig.3**

172 **Table 2.**

173 **Fractionations of soil organic carbon (SOC)**

174 The distribution of SOC and ¹⁴C-SOC in paddy soils after 45 days incubation are
175 characterized by either **physical** separation into different sizes or **chemical** separation
176 into different fractions based on solubility in alkali or acid. Soil organic carbon and
177 ¹⁴C-SOC **are** mainly detected in micro-aggregates (0.25–0.053 mm) and silt and clay
178 (< 0.053 mm) except for LZ and TY-B, while ¹⁴C-SOC **tends** to concentrate in
179 macro-aggregates compared to the small proportions in bulk soil (Fig. 4a). For the
180 chemical fractions, humins (HM) and fulvic acids (FA) dominate in bulk SOC, while
181 ¹⁴C-SOC concentrates mainly in HM for all samples (> 70%) (Fig. 4b)

182 **Fig. 4**

183 **Discussion**

184 Marker genes and microbes involved in **six** autotrophic pathways for atmospheric
185 CO₂ fixation in soils are detected and compared systematically for the first time in
186 paddy soils using metagenomic analyses. These genes are as abundant as other
187 genes involved in carbon, nitrogen, and sulfur cycling, arsenic metabolism, and
188 antibiotic resistance, etc. (Mackelprang et al., 2011; Xiao et al., 2016b; Xiao et al.,
189 2016a; Su et al., 2017). Results show that the Calvin cycle is the most abundant
190 pathway in paddy soils according to marker genes analysis (Fig. 1), while other
191 studies show that the reductive citric cycle dominates in desert soils (Liu et al., 2018),
192 and the reverse tricarboxylic acid cycle dominates in free-living microorganisms at
193 deep-sea hydrothermal vents (Campbell and Cary, 2004). **These results indicate** the
194 niche preference of different autotrophic metabolisms. **The genera carrying *cbbL* are**

195 similar to previous studies using the regular sanger-sequencing methods (Yuan et al.,
196 2012b; Xiao et al., 2014b), with phototrophs dominated by cyanobacteria, and
197 chemoautotrophs by microbes involved in sulfur, ammonia and iron oxidation (Tab.
198 S1). Results here also show that the marker genes associated with alternative
199 autotrophic pathways, other than the Calvin cycle, are ubiquitously found in paddy
200 soils (Fig. 1). There exists varied redox conditions in paddy soils, due to different
201 spatial and temporal conditions like rhizosphere vs. bulk soil, flooded vs. drained
202 conditions (Liesack et al., 2000), so genes and microbes associated with the rTCA
203 (mainly in micro-aerophiles and anaerobes) and especially the reductive acetyl-CoA
204 pathways (only in anaerobes) also exist in our samples. The 3-hydroxypropionate /
205 methyl-CoA cycle is poorly represented in the paddy soils, which is known to have
206 limited distribution due to the high energy cost involved in CO₂ assimilation (Berg,
207 2011). An important characteristic of this pathway is that it allows the co-assimilation
208 of numerous organic compounds, making it suitable for the mixotrophic microbes
209 (Zarzycki and Fuchs, 2011). The 4-hydroxypropionate cycle is only recently proposed
210 (Berg et al., 2007; Huber et al., 2008) and only found in archaea to date, however this
211 pathway is important in soils as it is lately found to be used by the *Thaumarchaea*, a
212 main ammonia oxidizer in soil (Zhang et al., 2010), as the data here also shows (Tab.
213 S1).

214 Results here show that autotrophic microbes are active and assimilate CO₂ into
215 MBC in paddy soils, which ultimately contributes to SOC (Fig. 3). In the work here
216 significant ¹⁴C₂ assimilation is detected only when soils are incubated in the light,
217 with almost no uptake when incubated in the dark (Yuan et al., 2012b; Ge et al., 2013),
218 suggesting that the microbial CO₂ assimilation processes are driven primarily by
219 autotrophs (including photo and chemoautotrophic microbes) in paddy soil. After 45
220 days incubation, 0.4-1.4% SOC and 6.7-15.1% MBC (data not shown) are labelled by
221 ¹⁴C, corresponding to turnover times of 8.8-30.3 years for SOC and 0.8-1.8 years for
222 MBC, assuming a net autotrophic metabolism in paddy soil. This shows that OC from

223 microbial CO₂ fixation can sustain a relatively fast turnover of microbial biomass in
224 paddy soil, but that this C tends to become more stable after partitioning into SOC. In
225 particular results show that more than 70% of the ¹⁴C-SOC concentrates in humins
226 (Fig. 4b), which are thought to be the least available for microbial degradation as they
227 are usually found to be strongly associated with soil minerals (Calace et al., 2007). In
228 support of this assertion there are significant positive correlations between clay
229 contents, total Fe and ¹⁴C-SOC in the paddy soils (Tab. 2), which is in line with the
230 growing evidence for the role of abiotic mechanisms, involving mineral sequestration
231 of SOC, in controlling SOC persistence in (Totsche et al., 2018; Hemingway et al.,
232 2019), with clay and iron oxides as the main minerals involved (Schweizer et al., 2019;
233 Wan et al., 2019). Soil microbes are also known to excrete extracellular polymeric
234 substance (EPS) (Cai et al., 2019), which play an important role in binding to soil
235 minerals and thus creating stable soil aggregates (Cai et al., 2018; Lin et al., 2018)
236 that help stabilize organic carbon in soil (Totsche et al., 2018). In our data, ¹⁴C-SOC
237 was distributed in different sizes of soil aggregate (Fig. 4a), suggesting that the
238 organic carbon from autotrophic CO₂ fixation contributes to the formation of soil
239 aggregates (Paerl and Priscu, 1998; Luo et al., 2019). It is also noteworthy that
240 organic carbon synthesized by autotrophs can be processed by heterotrophic
241 microbes and even virus and then transformed into MBC or SOC. For example, virus
242 in soil can lyse cell of autotrophs, releasing organics, which can be used by
243 heterotrophs, or transformed into more stable organic carbon (Liang and Balsler, 2011;
244 Schimel and Schaeffer, 2012; Liang et al., 2019; Bi et al., 2020). Taken together
245 multiple processes (like mineral protection, aggregation, and microbial transformation,
246 etc.) can strengthen the contribution of autotrophic metabolism to SOC accumulation
247 in paddy soils.

248 Paddy soil proves to be a reservoir of multiple autotrophic metabolisms (Fig. 1
249 and Tab. S1) and thus is an ideal natural laboratory for their study. In particular there
250 exists periodically changing redox conditions (oxic / anoxic) in paddy soil (Liesack et

251 al., 2000; Ge et al., 2012), so these might prove to be ideal environments to study the
252 role of oxygen on the evolution and diversification of autotrophic pathways, where
253 oxygen is thought to be one of the main controlling factors of these processes (Thauer,
254 2007; Ward and Shih, 2019). Autotrophic pathways emerged and diversified as a
255 result of oxygenation events during Earth history and key enzymes of many
256 autotrophic pathways show different sensitivities to oxygen, which directly determines
257 their distribution among microbes and in different environments (Berg, 2011). Some
258 microbes have more than one autotrophic pathway, like *Thioflavicoccus mobilis* which
259 possesses the genes for both the Calvin cycle and rTCA pathway (Tab. S1) (Markert
260 et al., 2007; Rubin-Blum et al., 2019) and the conditional usage of different CO₂
261 fixation pathways can be advantageous for this bacterial symbiont under fluctuating
262 redox conditions (Berg, 2011). The interplay between the Calvin cycle and rTCA cycle
263 in this bacterium may contribute to the high efficiency of carbon fixation under similar
264 conditions in paddy soils as well. Lastly, *Geobacter sulfurreducens*, a common
265 heterotrophic bacteria in paddy soil, is found to have a hidden chemolithoautotrophic
266 metabolism and can reduce CO₂ via the rTCA cycle after adaption in
267 chemolithoautotrophic growth medium containing Fe (III) and formate (Zhang et al.,
268 2020), implying hidden autotrophic potential in other common microbes. Therefore a
269 better understanding of these autotrophic metabolisms is needed, which is also
270 critical for management practices to increase SOC in the context of climate change
271 (Sá et al., 2017; Soussana et al., 2019).

272 In summary marker genes of six autotrophic pathways are detected in all paddy
273 samples using metagenomic analysis, which are dominated by the *cbbL* genes in the
274 Calvin cycle. Autotrophic microbes are active and assimilate 74.3 to 175.8 mg ¹⁴C kg⁻¹
275 into SOC and 5.2 to 24.1 mg ¹⁴C kg⁻¹ into MBC after 45 days incubation. Autotrophic
276 microbes contribute significantly to the stable organic carbon pool, where more than
277 70% of ¹⁴C-SOC was concentrated in the relatively stable humin fractions. Our work
278 highlights the importance of microbial CO₂ fixation to SOC accumulation in paddy

279 soils.

280

281 **Experimental procedures**

282 **Soil sampling and DNA extraction**

283 Top soil (0-20 cm) from five distinct sites in south China, Leizhou in Guangdong
284 Province (LZ), Jiaxing in Zhejiang Province(JX), Yingtan in Jiangxi Province (YT),
285 Gushi in Taoyuan (TY-G) and Baodongyu in Taoyuan (TY-B) in Hunan Province were
286 obtained. Rice is the main crop in these areas and diverse paddy soils develop from
287 different parent materials (Fig. S1). Physiochemical characteristics of the collected
288 soils are detailed in previous studies (Xiao et al., 2014b). To obtain sufficient DNA
289 from each of the five soil samples for metagenomic sequencing, DNA was extracted
290 from the five paddy soils (in duplicates) using the MoBio PowerSoil kit (MOBIO)
291 according to the manufacturer's protocol. DNA yields of 10 samples were between 1.0
292 and 2.5 ug, as quantified using the Quant-iT PicoGreen dsDNA HS assay kit
293 (Invitrogen) according to the manufacturer's manual.

294 **Sequencing and reads annotation**

295 DNA library preparation was performed according to the Illumina TruSeq DNA
296 sample preparation protocol. Each DNA sample was mechanically sheared by
297 Covaris M220 (Covaris). Libraries were then size-selected to about 300 bp.
298 Fragments were quantified using Agilent 2100 High Sensitivity DNA Assay (Agilent).
299 Sequencing was performed at Majorbio, Inc., Shanghai, China using Illumina HiSeq
300 2000 (Illumina) generating 2 x 101 bp paired end reads. [BBtools](https://sourceforge.net/projects/bbmap/)
301 (<https://sourceforge.net/projects/bbmap/>) was used to remove trace contaminants.
302 Raw reads were trimmed of adaptors and low quality reads using Sickle
303 (<https://github.com/najoshi/sickle>) and Seqprep (<https://github.com/jstjohn/SeqPrep>)
304 at default parameters, respectively. Low quality reads that contained ambiguous
305 nucleotides or had a quality value lower than 20 were removed (Chen et al., 2013).
306 The chimeric sequences were filtered out by UCHIME (Edgar et al., 2011). A total of

307 750,385,006 clean reads were generated across all 10 samples with an average of
308 75,038,500 reads per sample. Data are available at the NCBI Short Read Archive
309 under accession number SRA023560.

310 To facilitate the annotation speed, nucleotide and amino acid sequences of
311 targeted KEGG Orthologies (KO) of five marker genes (K01601 *cbbL*, K15230 *acIA*,
312 K00198 *acsA*, K01962 *accA* and K14534 *hcd*) involved in microbial CO₂ fixation
313 pathways were extracted from the KEGG database and used as a subject database
314 for analysis. These sequences were reviewed with high quality and strictness, which
315 had to be confirmed by case studies already, and only the complete open reading
316 frame (ORF) sequences were included. The local BLASTX programs were employed
317 to align clean reads of each data set to the subject database with e value 1×10^{-5} ,
318 similarity > 90%, and aligned amino acids length > 25 (Cai et al., 2013; Xiao et al.,
319 2016a). The relative abundance of each gene was determined as hit numbers divided
320 by total number of reads (ppm, one read in one million reads). Marker genes
321 associated microbes were defined as microbes of aligned sequenced and
322 summarized at genus level. Microbial community diversity was quantified using
323 Shannon–Weiner diversity index (H, e as bases), as listed in Table 1. Similarity matrix
324 of microbial co-occurrence network was calculated using Spearman correlation in R
325 (<https://personality-project.org/r/psych>). Co-occurrence network was visualized by
326 Gephi (Bastian et al., 2009), with cut-off values correlation coefficient > 0.6 and false
327 discovery rate (FDR) corrected ($P < 0.01$).

328 **Incubation with ¹⁴C-labeled CO₂**

329 One set of microcosms of the five soils, each with four replicates, were prepared
330 by weighing 500 g (on an oven-dried basis) of fresh soil into PVC plastic tubes (20 cm
331 diameter × 15 cm height). All PVC columns were incubated in a growth chamber (80 ×
332 200 cm, height 120 cm) for 45 days with continuous ¹⁴C-CO₂ labeling as described
333 previously (Ge et al., 2013; Wu et al., 2015). The ¹⁴C-CO₂ was generated by forcing a
334 ¹⁴C-Na₂CO₃ solution (1.0 M, a radioactivity of 1.68×10^4 Bq μg⁻¹ C) into an acid bath

335 (HCl, 2 M) and giving a concentration from 360 and 380 $\mu\text{L L}^{-1}$ (Shsen-QZD, Qingdao,
336 China). Two temperature humidity sensors (SNT-96S, Qingdao, China) were installed:
337 one inside the chamber, and another in the surrounding rice field in the open air. An
338 air-conditioning system was used to control the temperature inside the chamber within
339 1°C from ambient temperature in the field (outside). Two fans continuously circulated
340 the atmosphere in the growth chamber. The incubation chamber system was placed
341 outdoors in order to maintain natural exposure to sunlight (Ge et al., 2014), as there
342 was almost no uptake of $^{14}\text{CO}_2$ when incubated in the dark (Yuan et al., 2012b; Ge et
343 al., 2013). The paddy soils were permanently flooded (2-3 cm water layer) by the
344 addition of sterile distilled water as required during the incubation span. At the end of
345 the 45 days incubation, soils were removed from the microcosms, mixed thoroughly
346 then divided into two separate portions. One portion was oven-dried at 70°C to a
347 constant weight to determine the amount of ^{14}C -SOC fixed from $^{14}\text{CO}_2$, and the other
348 was stored at 4°C to determine ^{14}C -MBC. The synthesis rates (RS) of ^{14}C -SOC (RS, g
349 $\text{C m}^{-2} \text{d}^{-1}$) were calculated using the formula: $\text{RS} = ^{14}\text{C-SOC} * (1/(3.14 * (D/2)^2)) / T$,
350 where D represents the internal diameter of the container (m) and T, the incubation
351 time (45 d) respectively.

352 **Soil partition and ^{14}C radioactivity analysis**

353 Soil aggregate size fractionation was performed by the wet sieving method (Gale
354 et al., 2000). Briefly, air-dried soil was sieved through 8 mm mesh and was gently
355 crumbled manually to approximately 2 mm pieces. A 100 g soil sample was
356 transferred to two sieves (0.25 and 0.053 mm) and shaken for 5 min. Subsequently,
357 macro-aggregates (2–0.25 mm) and micro-aggregates (0.25–0.053 mm) were
358 collected from the 0.25 mm and 0.053 mm sieves, respectively. The remaining
359 material that passed through the 0.053 mm sieve was classified as silt and clay (<
360 0.053 mm). All size fractions were dried at 70°C , weighed, and stored for ^{14}C analysis.
361 The extraction of SOC pools from air-dried soil was performed using the methodology
362 recommended by the International Humic Substances Society (IHSS), using

363 NaOH-Na₄P₂O₇·10H₂O (0.1 M, pH = 13) as the extraction agent (Swift, 1996). Three
364 fractions were separated from 5 g soil samples based on their solubility in alkaline and
365 acid solutions, and separated into three fractions: (a) alkali- and acid-extractable fulvic
366 acids (FAs); (b) alkali-extractable, acid non-extractable humic acids (HAs); and (3)
367 alkali and acid non-extractable humin (HM). For ¹⁴C analysis, 3.0 ml 2.5 M HCl was
368 added and mixed with 1.50 g of soil (sieved with a mesh < 0.149 mm) (v: w = 2: 1) in
369 Dophin tubes for 24 hours to remove inorganic carbon (such as CaCO₃ in soil
370 samples). Then, the aliquots were washed twice with 3.0 ml H₂O to remove any
371 remaining HCl (Theis et al., 2007) before measuring ¹⁴C-SOC. After that, 1.50 g
372 inorganic carbon-removed soil was digested with a mixture of K₂Cr₂O₇ and
373 concentrated H₂SO₄-H₃PO₄, as described by Ge *et al.* (2013). ¹⁴C-MBC measurement
374 was performed based on the fumigation-extraction method and was determined using
375 K₂SO₄ extracts (Wu and O'Donnell, 1997), and the ¹⁴C radioactivity was measured
376 using an automated liquid scintillation counter (LS-6500, Beckman, Germany). The
377 ¹⁴C-SOC and ¹⁴C-MBC amounts were calculated according to the procedure
378 described by Ge *et al.* (2013). Full details are given in previous studies of the
379 co-author groups (Ge et al., 2013; Wu et al., 2014; Wu et al., 2015).

380 **Statistical analysis**

381 All data are expressed as the mean ± standard error (or deviation). Differences
382 between means were evaluated by one-way analysis of variance (ANOVA) [after](#)
383 [normal distribution test](#). Correlation analyses were carried out using the [Spearman](#)
384 correlation method. Significance was defined at the 0.05 level unless otherwise stated.
385 All analyses were performed using SPSS 18.0.

386

387 **Acknowledgements**

388 This work was supported by National Science Foundation of China (Grant 41090282,
389 Grant 41977038 and Grant 41950410565), Key Projects of Natural Science
390 Foundation of China (Grant 41090280), Hunan Province Base for Scientific and

391 Technological Innovation Cooperation (2018WK4012), the Youth Innovation Team
392 Project of Institute of Subtropical Agriculture, Chinese Academy of Sciences
393 (2017QNCXTD_GTD), National Natural Science Foundation of Hunan Province
394 (2019JJ10003 and 2019JJ30028), and NERC Highlight Topic Grant (NE/S004963/1
395 Locked Up). In addition, this research project has received funding from the European
396 Research Council (ERC) under the European Union's Horizon 2020 research and
397 innovation programme (Grant agreement No. 725613 MinOrg).

398

399 **Competing of Interests**

400 The authors declare no competing interests.

401

402 **References**

403 Alfreider, A., Vogt, C., Hoffmann, D., and Babel, W. (2003) Diversity of
404 ribulose-1,5-bisphosphate carboxylase/oxygenase large-subunit genes from
405 groundwater and aquifer microorganisms. *Microbial Ecol* **45**: 317-328.

406 Anantharaman, K., Brown, C.T., Hug, L.A., Sharon, I., Castelle, C.J., Probst, A.J. et
407 al. (2016) Thousands of microbial genomes shed light on interconnected
408 biogeochemical processes in an aquifer system. *Nat Commun* **7**: 13219.

409 Bassham, J.A., Benson, A.A., and Calvin, M. (1950) The pathway of carbon in
410 photosynthesis. *J Biol Chem* **185**: 781-788.

411 Bastian, M., Heymann, S., and Jacomy, M. (2009) *Gephi: An Open Source Software*
412 *for Exploring and Manipulating Networks*.

413 Berg, I.A. (2011) Ecological aspects of the distribution of different autotrophic CO₂
414 fixation pathways. *Appl Environ Microbiol* **77**: 1925-1936.

- 415 Berg, I.A., Kockelkorn, D., Buckel, W., and Fuchs, G. (2007) A
416 3-hydroxypropionate/4-hydroxybutyrate autotrophic carbon dioxide assimilation
417 pathway in archaea. *Science* **318**: 1782-1786.
- 418 Bi, L., Yu, D.T., Du, S., Zhang, L.M., Zhang, L.Y., Wu, C.F. et al. (2020) Diversity and
419 potential biogeochemical impacts of viruses in bulk and rhizosphere soils. *Environ*
420 *Microbiol n/a*.
- 421 Cai, L., Yu, K., Yang, Y., Chen, B.-w., Li, X.-d., and Zhang, T. (2013) Metagenomic
422 exploration reveals high levels of microbial arsenic metabolism genes in activated
423 sludge and coastal sediments. *Appl Microbiol Biol* **97**: 9579-9588.
- 424 Cai, P., Lin, D., Peacock, C.L., Peng, W., and Huang, Q. (2018) EPS adsorption to
425 goethite: Molecular level adsorption mechanisms using 2D correlation spectroscopy.
426 *Chem Geol* **494**: 127-135.
- 427 Cai, P., Sun, X., Wu, Y., Gao, C., Mortimer, M., Holden, P.A. et al. (2019) Soil
428 biofilms: microbial interactions, challenges, and advanced techniques for ex-situ
429 characterization. *Soil Ecology Letters* **1**: 85-93.
- 430 Calace, N., Petronio, B.M., Persia, S., Pietroletti, M., and Pacioni, D. (2007) A new
431 analytical approach for humin determination in sediments and soils. *Talanta* **71**:
432 1444-1448.
- 433 Campbell, B.J., and Cary, S.C. (2004) Abundance of reverse tricarboxylic acid cycle
434 genes in free-living microorganisms at deep-sea hydrothermal vents. *Appl Environ*
435 *Microbiol* **70**: 6282-6289.
- 436 Campbell, B.J., Stein, J.L., and Cary, S.C. (2003) Evidence of chemolithoautotrophy

- 437 in the bacterial community associated with *Alvinella pompejana*, a hydrothermal vent
438 polychaete. *Appl Environ Microbiol* **69**: 5070-5078.
- 439 Chen, B., Yang, Y., Liang, X., Yu, K., Zhang, T., and Li, X. (2013) Metagenomic
440 profiles of antibiotic resistance genes (ARGs) between human impacted estuary and
441 deep ocean sediments. *Environ Sci Technol* **47**: 12753-12760.
- 442 Davidson, E.A., and Janssens, I.A. (2006) Temperature sensitivity of soil carbon
443 decomposition and feedbacks to climate change. *Nature* **440**: 165-173.
- 444 Dincher, M., Calvaruso, C., and Turpault, M.-P. (2020) Major element residence times
445 in humus from a beech forest: The role of element forms and recycling. *Soil Biol
446 Biochem* **141**: 107674.
- 447 Edgar, R.C., Haas, B.J., Clemente, J.C., Quince, C., and Knight, R. (2011) UCHIME
448 improves sensitivity and speed of chimera detection. *Bioinformatics* **27**: 2194-2200.
- 449 Evans, M.C., Buchanan, B.B., and Arnon, D.I. (1966) A new ferredoxin-dependent
450 carbon reduction cycle in a photosynthetic bacterium. *Proc Natl Acad Sci U S A* **55**:
451 928-934.
- 452 Gale, W.J., Cambardella, C.A., and Bailey, T.B. (2000) Root-derived carbon and the
453 formation and stabilization of aggregates. *Soil Sci Soc Am J* **64**: 201-207.
- 454 Ge, T., Liu, C., Yuan, H., Zhao, Z., Wu, X., Zhu, Z. et al. (2014) Tracking the
455 photosynthesized carbon input into soil organic carbon pools in a rice soil fertilized
456 with nitrogen. *Plant Soil* **392**: 17-25.
- 457 Ge, T., Yuan, H., Zhu, H., Wu, X., Nie, S.a., Liu, C. et al. (2012) Biological carbon
458 assimilation and dynamics in a flooded rice – Soil system. *Soil Biol Biochem* **48**:

- 459 39-46.
- 460 Ge, T., Wu, X., Chen, X., Yuan, H., Zou, Z., Li, B. et al. (2013) Microbial phototrophic
461 fixation of atmospheric CO₂ in China subtropical upland and paddy soils. *Geochim*
462 *Cosmochim Acta* **113**: 70-78.
- 463 Hemingway, J.D., Rothman, D.H., Grant, K.E., Rosengard, S.Z., Eglinton, T.I., Derry,
464 L.A., and Galy, V.V. (2019) Mineral protection regulates long-term global preservation
465 of natural organic carbon. *Nature* **570**: 228-231.
- 466 Holo, H. (1989) *Chloroflexus aurantiacus* secretes 3-hydroxypropionate, a possible
467 intermediate in the assimilation of CO₂ and acetate. *Arch Microbiol* **151**: 252-256.
- 468 Huber, H., Gallenberger, M., Jahn, U., Eylert, E., Berg, I.A., Kockelkorn, D. et al.
469 (2008) A dicarboxylate/4-hydroxybutyrate autotrophic carbon assimilation cycle in the
470 hyperthermophilic Archaeum *Ignicoccus hospitalis*. *Proc Natl Acad Sci U S A* **105**:
471 7851-7856.
- 472 Hultman, J., Waldrop, M.P., Mackelprang, R., David, M.M., McFarland, J., Blazewicz,
473 S.J. et al. (2015) Multi-omics of permafrost, active layer and thermokarst bog soil
474 microbiomes. *Nature* **521**: 208-212.
- 475 Janzen, H.H. (2004) Carbon cycling in earth systems—a soil science perspective. *Agr*
476 *Ecosyst Environ* **104**: 399-417.
- 477 Kallenbach, C.M., Frey, S.D., and Grandy, A.S. (2016) Direct evidence for
478 microbial-derived soil organic matter formation and its ecophysiological controls. *Nat*
479 *Commun* **7**: 13630.
- 480 Kapkiyai, J.J., Karanja, N.K., Qureshi, J.N., Smithson, P.C., and Woomeer, P.L. (1999)

- 481 Soil organic matter and nutrient dynamics in a Kenyan nitisol under long-term fertilizer
482 and organic input management. *Soil Biol Biochem* **31**: 1773-1782.
- 483 Lal, R. (2008) Carbon sequestration. *Philos T Roy Soc B* **363**: 815-830.
- 484 Lam, K.N., Cheng, J., Engel, K., Neufeld, J.D., and Charles, T.C. (2015) Current and
485 future resources for functional metagenomics. *Front Microbiol* **6**.
- 486 Lehmann, J., and Kleber, M. (2015) The contentious nature of soil organic matter.
487 *Nature* **528**: 60.
- 488 Lever, M.A. (2013) Functional gene surveys from ocean drilling expeditions – a review
489 and perspective. *FEMS Microbiol Ecol* **84**: 1-23.
- 490 Liang, C., and Balsler, T.C. (2011) Microbial production of recalcitrant organic matter
491 in global soils: implications for productivity and climate policy. *Nat Rev Micro* **9**: 75-75.
- 492 Liang, C., Schimel, J.P., and Jastrow, J.D. (2017) The importance of anabolism in
493 microbial control over soil carbon storage. *Nat Microbiol* **2**: 17105.
- 494 Liang, C., Amelung, W., Lehmann, J., and Kastner, M. (2019) Quantitative
495 assessment of microbial necromass contribution to soil organic matter. *Glob Chang*
496 *Biol* **25**: 3578-3590.
- 497 Liesack, W., Schnell, S., and Revsbech, N.P. (2000) Microbiology of flooded rice
498 paddies. *FEMS Microbiol Rev* **24**: 625-645.
- 499 Lin, D., Cai, P., Peacock, C.L., Wu, Y., Gao, C., Peng, W. et al. (2018) Towards a
500 better understanding of the aggregation mechanisms of iron (hydr)oxide nanoparticles
501 interacting with extracellular polymeric substances: Role of pH and electrolyte
502 solution. *Sci Total Environ* **645**: 372-379.

- 503 Liu, J., Kong, W., Zhang, G., Khan, A., Guo, G., Zhu, C. et al. (2016) Diversity and
504 succession of autotrophic microbial community in high-elevation soils along
505 deglaciation chronosequence. *FEMS Microbiol Ecol* **92**.
- 506 Liu, Z., Sun, Y., Zhang, Y., Feng, W., Lai, Z., Fa, K., and Qin, S. (2018) Metagenomic
507 and ¹³C tracing evidence for autotrophic atmospheric carbon absorption in a semiarid
508 desert. *Soil Biol Biochem* **125**: 156-166.
- 509 Luo, Y., Zhu, Z., Liu, S., Peng, P., Xu, J., Brookes, P. et al. (2019) Nitrogen
510 fertilization increases rice rhizodeposition and its stabilization in soil aggregates and
511 the humus fraction. *Plant Soil* **445**: 125-135.
- 512 Ma, B., Zhao, K., Lv, X., Su, W., Dai, Z., Gilbert, J.A. et al. (2018) Genetic correlation
513 network prediction of forest soil microbial functional organization. *ISME J* **12**:
514 2492-2505.
- 515 Mackelprang, R., Waldrop, M.P., DeAngelis, K.M., David, M.M., Chavarria, K.L.,
516 Blazewicz, S.J. et al. (2011) Metagenomic analysis of a permafrost microbial
517 community reveals a rapid response to thaw. *Nature* **480**: 368-371.
- 518 Markert, S., Arndt, C., Felbeck, H., Becher, D., Sievert, S.M., Hügler, M. et al. (2007)
519 Physiological proteomics of the uncultured endosymbiont of *Riftia pachyptila*. *Science*
520 **315**: 247.
- 521 Metcalf, J.L., Xu, Z.Z., Weiss, S., Lax, S., Van Treuren, W., Hyde, E.R. et al. (2016)
522 Microbial community assembly and metabolic function during mammalian corpse
523 decomposition. *Science* **351**: 158-162.
- 524 Newman, M.E.J. (2006) Modularity and community structure in networks. *Proc Natl*

- 525 *Acad Sci U S A* **103**: 8577.
- 526 Paerl, H.W., and Priscu, J.C. (1998) Microbial phototrophic, heterotrophic, and
527 diazotrophic activities associated with aggregates in the permanent ice cover of Lake
528 Bonney, Antarctica. *Microbial Ecol* **36**: 221-230.
- 529 Rubin-Blum, M., Dubilier, N., and Kleiner, M. (2019) Genetic evidence for two carbon
530 fixation pathways (the Calvin-Benson-Bassham cycle and the reverse tricarboxylic
531 acid cycle) in symbiotic and free-living bacteria. *mSphere* **4**: e00394-00318.
- 532 Sá, J.C.d.M., Lal, R., Cerri, C.C., Lorenz, K., Hungria, M., and de Faccio Carvalho,
533 P.C. (2017) Low-carbon agriculture in South America to mitigate global climate
534 change and advance food security. *Environ Int* **98**: 102-112.
- 535 Schimel, J., and Schaeffer, S. (2012) Microbial control over carbon cycling in soil.
536 *Front Microbiol* **3**.
- 537 Schmidt, M.W.I., Torn, M.S., Abiven, S., Dittmar, T., Guggenberger, G., Janssens,
538 I.A. et al. (2011) Persistence of soil organic matter as an ecosystem property. *Nature*
539 **478**: 49-56.
- 540 Schweizer, S.A., Bucka, F.B., Graf-Rosenfellner, M., and Kögel-Knabner, I. (2019)
541 Soil microaggregate size composition and organic matter distribution as affected by
542 clay content. *Geoderma* **355**: 113901.
- 543 Selesi, D., Schmid, M., and Hartmann, A. (2005) Diversity of green-like and red-like
544 ribulose-1,5-bisphosphate carboxylase/oxygenase large-subunit genes (*cbbL*) in
545 differently managed agricultural soils. *Appl Environ Microbiol* **71**: 175-184.
- 546 Simpson, A.J., Simpson, M.J., Smith, E., and Kelleher, B.P. (2007) Microbially derived

- 547 inputs to soil organic matter: are current estimates too low? *Environ Sci Technol* **41**:
548 8070-8076.
- 549 Soussana, J.-F., Luffalla, S., Ehrhardt, F., Rosenstock, T., Lamanna, C., Havlík, P. et
550 al. (2019) Matching policy and science: Rationale for the '4 per 1000 - soils for food
551 security and climate' initiative. *Soil Till Res* **188**: 3-15.
- 552 Su, J.-Q., Xia, Y., Yao, H.-Y., Li, Y.-Y., An, X.-L., Singh, B.K. et al. (2017)
553 Metagenomic assembly unravel microbial response to redox fluctuation in acid sulfate
554 soil. *Soil Biol Biochem* **105**: 244-252.
- 555 Swift, R.S. (1996) Organic matter characterization. In *Methods of Soil Analysis*. D.L.
556 Sparks, A.L.P., P.A. Helmke, R.H. Loeppert, P. N. Soltanpour, M. A. Tabatabai,
557 C. T. Johnston, M. E. Sumner (ed). No. 5, Madison, WI, USA: Soil Science Society of
558 America.
- 559 Thauer, R.K. (2007) A fifth pathway of carbon fixation. *Science* **318**: 1732-1733.
- 560 Theis, D.E., Jaeggi, M., Aeschlimann, D., Blum, H., Frossard, E., and Siegwolf,
561 R.T.W. (2007) Dynamics of soil organic matter turnover and soil respired CO₂ in a
562 temperate grassland labelled with ¹³C. *Eur J Soil Sc* **58**: 1364-1372.
- 563 Totsche, K.U., Amelung, W., Gerzabek, M.H., Guggenberger, G., Klumpp, E., Knief,
564 C. et al. (2018) Microaggregates in soils. *J Plant Nutr Soil Sci* **181**: 104-136.
- 565 Tyson, G.W., Chapman, J., Hugenholtz, P., Allen, E.E., Ram, R.J., Richardson, P.M.
566 et al. (2004) Community structure and metabolism through reconstruction of microbial
567 genomes from the environment. *Nature* **428**: 37-43.
- 568 Venter, J.C., Remington, K., Heidelberg, J.F., Halpern, A.L., Rusch, D., Eisen, J.A. et

- 569 al. (2004) Environmental genome shotgun sequencing of the Sargasso Sea. *Science*
570 **304**: 66.
- 571 Wan, D., Ye, T.H., Lu, Y., Chen, W.L., Cai, P., and Huang, Q.Y. (2019) Iron oxides
572 selectively stabilize plant-derived polysaccharides and aliphatic compounds in
573 agricultural soils. *Eur J Soil Sc* **0**.
- 574 Ward, L.M., and Shih, P.M. (2019) The evolution and productivity of carbon fixation
575 pathways in response to changes in oxygen concentration over geological time. *Free*
576 *Radic Biol Med* **140**: 188-199.
- 577 Wood, H.G., Ragsdale, S.W., and Pezacka, E. (1986) The acetyl-CoA pathway: a
578 newly discovered pathway of autotrophic growth. *Trends Biochem Sci* **11**: 14-18.
- 579 Wu, J., and O'Donnell, A.G. (1997) Procedure for the simultaneous analysis of total
580 and radioactive carbon in soil and plant materials. *Soil Biol Biochem* **29**: 199-202.
- 581 Wu, X., Ge, T., Wang, W., Yuan, H., Wegner, C.E., Zhu, Z. et al. (2015) Cropping
582 systems modulate the rate and magnitude of soil microbial autotrophic CO₂ fixation in
583 soil. *Front Microbiol* **6**: 379.
- 584 Wu, X., Ge, T., Yuan, H., Li, B., Zhu, H., Zhou, P. et al. (2014) Changes in bacterial
585 CO₂ fixation with depth in agricultural soils. *Appl Microbiol Biol* **98**: 2309-2319.
- 586 Xiao, K.-Q., Nie, S.-A., Bao, P., Wang, F.-H., Bao, Q.-L., and Zhu, Y.-G. (2014a)
587 Rhizosphere effect has no effect on marker genes related to autotrophic CO₂ fixation
588 in paddy soils? *J Soils Sediments* **14**: 1082-1087.
- 589 Xiao, K.-Q., Bao, P., Bao, Q.-L., Jia, Y., Huang, F.-Y., Su, J.-Q., and Zhu, Y.-G.
590 (2014b) Quantitative analyses of ribulose-1,5-bisphosphate carboxylase/oxygenase

- 591 (RubisCO) large-subunit genes (*cbbL*) in typical paddy soils. *FEMS Microbiol Ecol* **87**:
592 89-101.
- 593 Xiao, K.-Q., Li, L.-G., Ma, L.-P., Zhang, S.-Y., Bao, P., Zhang, T., and Zhu, Y.-G.
594 (2016a) Metagenomic analysis revealed highly diverse microbial arsenic metabolism
595 genes in paddy soils with low-arsenic contents. *Environ Pollut* **211**: 1-8.
- 596 Xiao, K.-Q., Li, B., Ma, L., Bao, P., Zhou, X., Zhang, T., and Zhu, Y.-G. (2016b)
597 Metagenomic profiles of antibiotic resistance genes in paddy soils from South China.
598 *FEMS Microbiol Ecol* **92**.
- 599 Yuan, H.-Z., Ge, T.-D., Chen, C.-Y., O'Donnell, A.G., and Wu, J.-S. (2012a)
600 Significant role for microbial autotrophy in the sequestration of soil carbon. *Appl*
601 *Environ Microbiol* **78**: 2328-2336.
- 602 Yuan, H., Ge, T., Chen, C., O'Donnell, A.G., and Wu, J. (2012b) Significant role for
603 microbial autotrophy in the sequestration of soil carbon. *Appl Environ Microbiol* **78**:
604 2328-2336.
- 605 Zarzycki, J., and Fuchs, G. (2011) Coassimilation of organic substrates via the
606 autotrophic 3-hydroxypropionate bi-cycle in *Chloroflexus aurantiacus*. *Appl Environ*
607 *Microbiol* **77**: 6181.
- 608 Zhang, L.-M., Offre, P.R., He, J.-Z., Verhamme, D.T., Nicol, G.W., and Prosser, J.I.
609 (2010) Autotrophic ammonia oxidation by soil thaumarchaea. *Proc Natl Acad Sci U S*
610 *A* **107**: 17240.
- 611 Zhang, T., Shi, X.C., Ding, R., Xu, K., and Tremblay, P.L. (2020) The hidden
612 chemolithoautotrophic metabolism of *Geobacter sulfurreducens* uncovered by

613 adaptation to formate. *ISME J.*

For Peer Review Only

615 **Table and Figure legends**

616

617 **Table 1** Shannon–Wiener index of marker genes associated microbes.

	<i>cbbL</i>	<i>aclA</i>	<i>acsA</i>	<i>accA</i>	<i>hcd</i>
LZ	3.43	0.25	2.06	0.59	0.96
JX	3.53	0.07	2.59	0.92	0.79
YT	3.60	0.22	2.41	0.6	0.81
TY-G	3.43	0.09	2.31	0.66	0.86
TY-B	3.45	0.07	2.15	0.51	0.87

618

619 **Table 2.** Correlation of soil properties and marker genes with amounts of ¹⁴C-SOC620 and ¹⁴C-MBC in paddy soils after 45 d incubation.

	¹⁴ C-SOC	¹⁴ C-MBC
Soil properties		
pH	0.23	0.03
Total C	-0.76	0.76
Total N	-0.75	0.54
SOC	-0.73	0.78
DOC	-0.02	0.70
Total Fe	0.93*	-0.25
Total Mn	0.79	0.20
clay	0.93*	-0.27
silt	-0.80	0.08
sand	-0.90*	0.59
Gene abundance		
<i>cbbL</i>	0.90*	-0.36
<i>aclA</i>	-0.65	-0.38
<i>acsA</i>	0.37	-0.26
<i>accA</i>	0.23	-0.68
<i>hcd</i>	0.05	-0.81

621 *Correlation is significant at the 0.05 level (2-tailed).

622

624 **Fig. 1** Abundances of marker genes of six autotrophic pathways in five paddy soils
625 from South China, (a) abundance ppm, one read in one million reads, error bars
626 indicate the standard deviation of the mean ($n = 2$), (b) relative abundance
627 percentages (%) of five marker genes. *cbbL* (ribulose-bisphosphate carboxylase large
628 chain), *acIA* (ATP-citrate lyase alpha-subunit), *acsA* (carbon-monoxide
629 dehydrogenase catalytic subunit), *accA* (acetyl-CoA carboxylase carboxyl transferase
630 subunit alpha), *hcd* (4-hydroxybutyryl-CoA dehydratase). LZ, Leizhou in Guangdong
631 Province; JX, Jiaying in Zhejiang Province; YT, Yingtian in Jiangxi Province; TY-G,
632 Gushi of Taoyuan in Hunan Province; TY-B, Baodongyu of Taoyuan in Hunan
633 Province. Abbreviations apply to all figures and tables in the followings.

634

635 **Fig. 2** Network of co-occurring autotrophic microbes (genera) of six pathways in
636 paddy soils based on correlation analysis. The size of each node is proportional to the
637 number of connections (that is, degree), and the colors of nodes denote microbes
638 from different pathways: the Calvin cycle (I), the reductive tricarboxylic acid (rTCA)
639 cycle (II), the reductive acetyl-CoA pathway (III), the 3-hydroxypropionate / methyl-CoA
640 cycle (IV) and the 4-hydroxybutyrate cycle (V). The width of each edge is proportional
641 to the weight and the colors of edge denote positive (pink) or negative (light blue)
642 connection.

643

644 **Fig.3** The amounts of ^{14}C -SOC, ^{14}C -MBC (a) and the synthesis rates of ^{14}C -SOC (b)
645 in five paddy soils incubated in a growth chamber with $^{14}\text{CO}_2$ for 45 d. Error bars
646 indicate the standard error of the mean ($n = 4$) and means with the same letter are not
647 significantly different among different soils ($P > 0.05$).

648

649 **Fig. 4** Fractionation of soil organic carbon (SOC) in five paddy soils, (a) distribution of
650 SOC and ^{14}C -SOC in different sizes of soil aggregates, (b) distribution of SOC and

651 ^{14}C -SOC in different chemical fractions of soil, HM for humins, HA for humic acids and
652 FA for fulvic acids.

For Peer Review Only

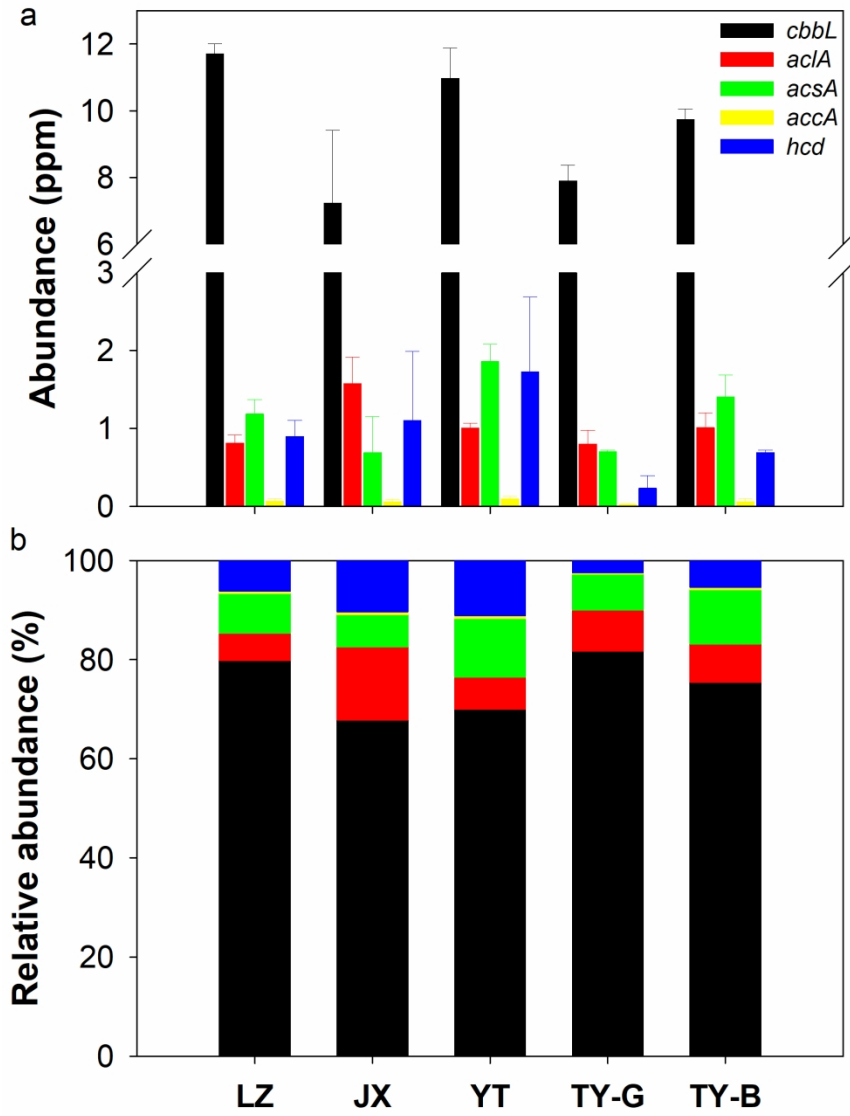


Fig. 1

172x215mm (300 x 300 DPI)

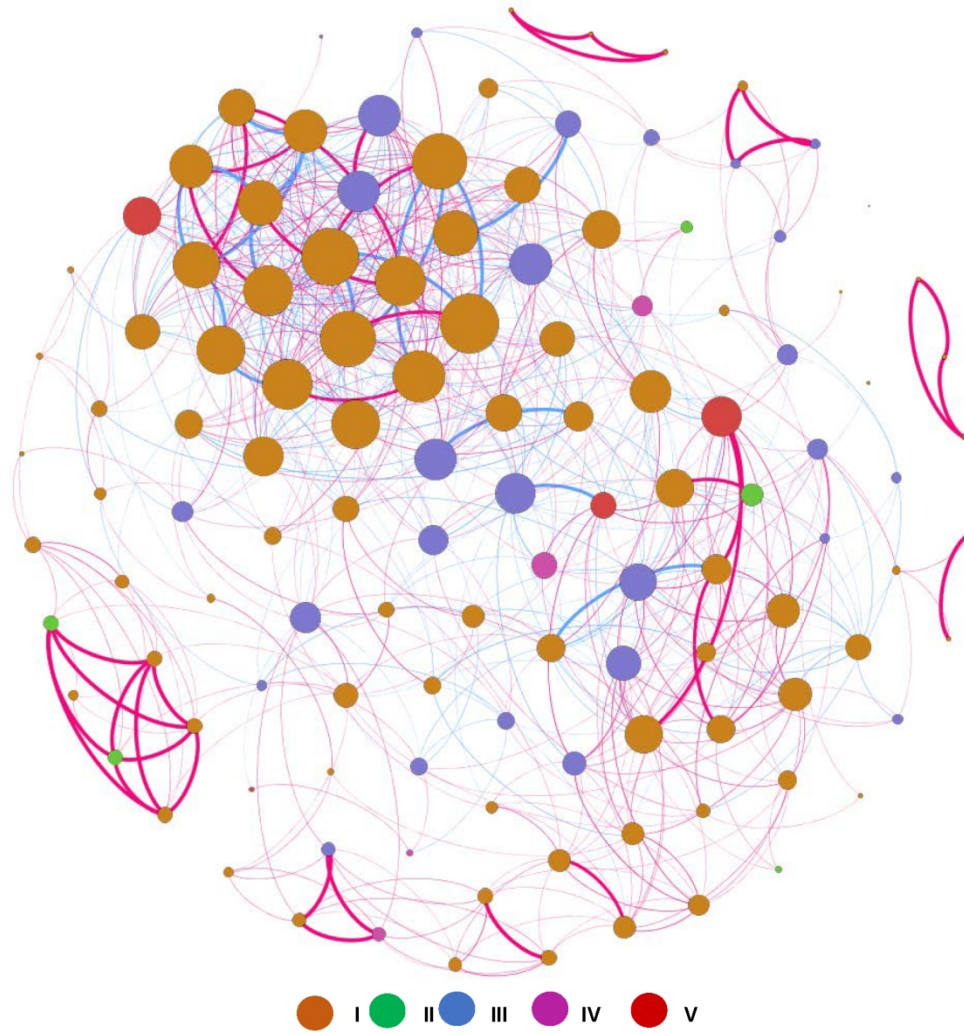


Fig. 2

143x149mm (300 x 300 DPI)

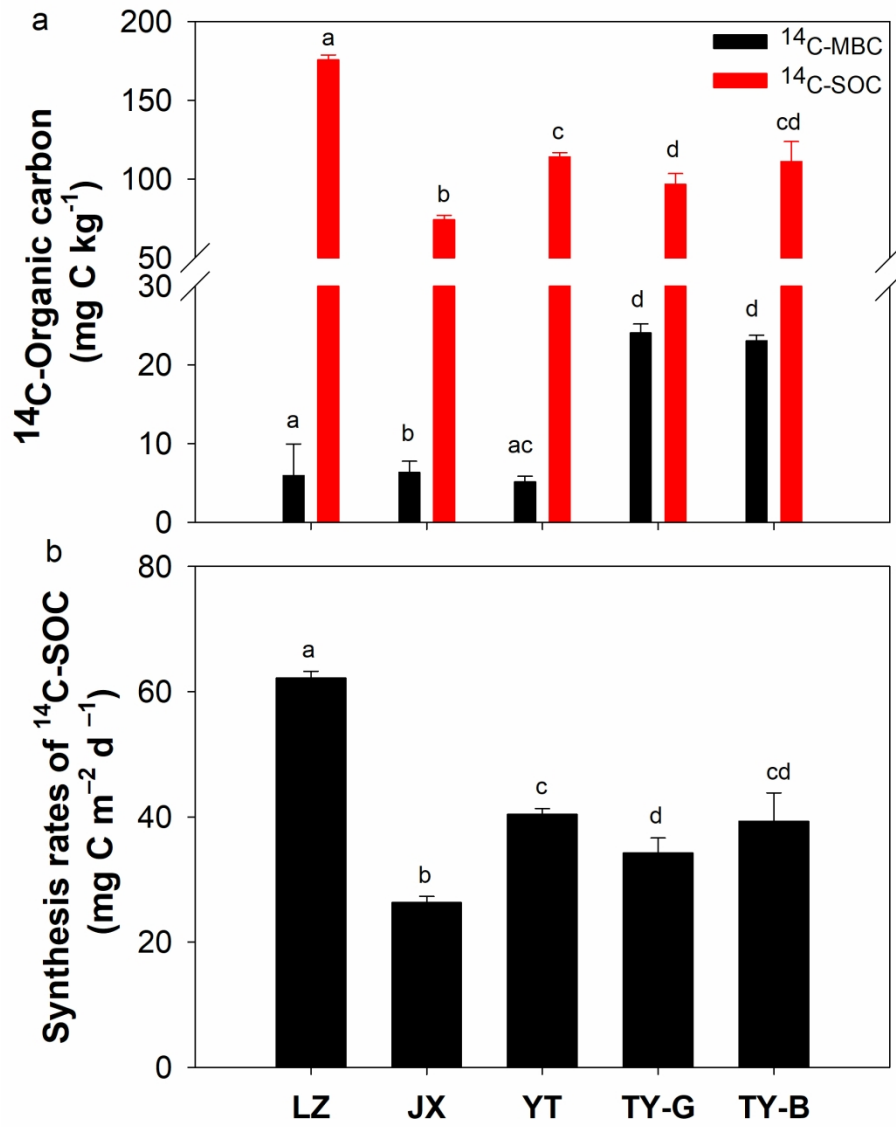


Fig. 3

167x215mm (300 x 300 DPI)

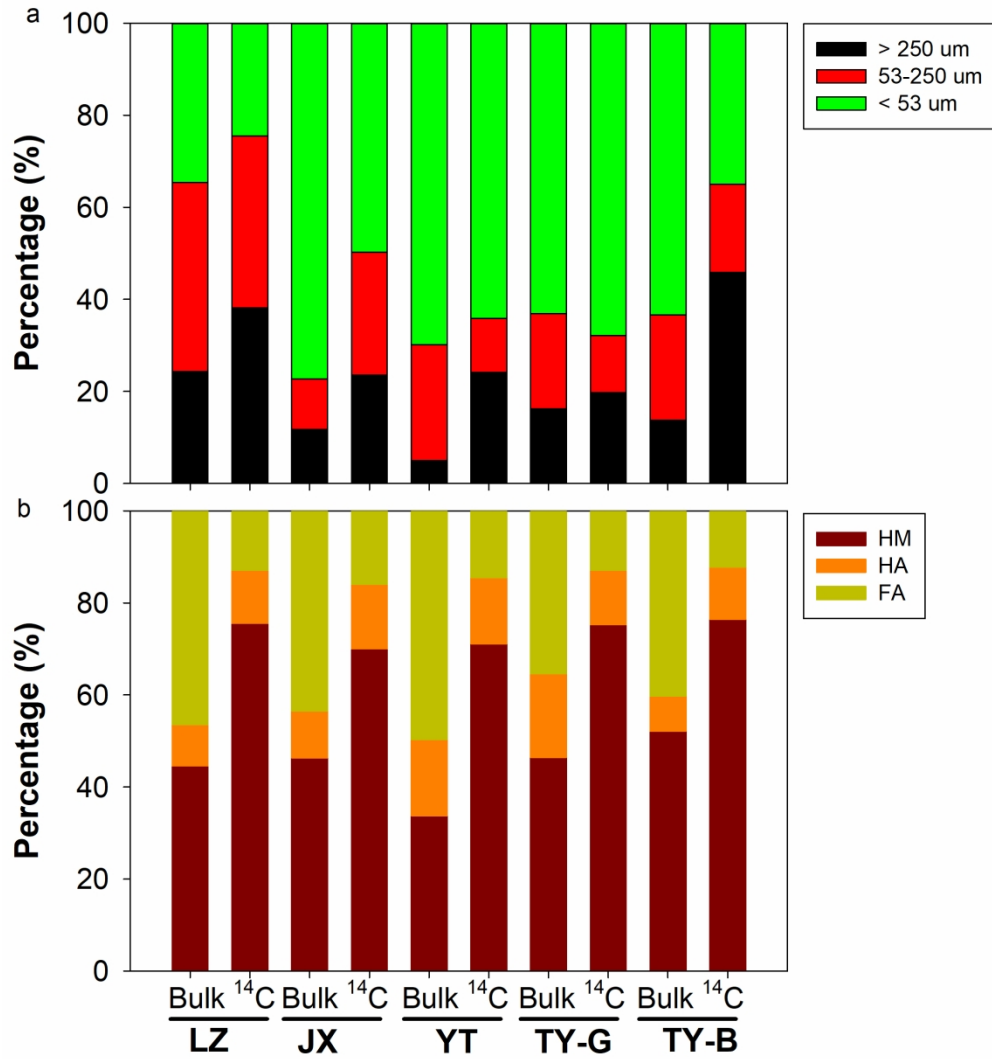


Fig. 4

193x214mm (300 x 300 DPI)